BULLETIN

OF THE

KOREAN CHEMICAL SOCIETY

ISSN 0253-2964 BKCSDE 23(5) 643-782
Volume 23, Number 5 May 20, 2002

Feature Article

Synthesis and Catalytic Properties of Imidazole-Functionalized Poly(propylene imine) Dendrimers

Lane A. Baker,[1] Li Sun, and Richard M. Crooks*

Department of Chemistry, Texas A&M University, P.O. Box 30012, College Station, TX 77842-3012, USA
Received December 27, 2001

The synthesis and characterization of third- and fifth-generation poly(propylene imine) dendrimers terminated with imidazole moieties is reported. Functionalization was achieved using simple peptide coupling reagents. These materials were characterized by MALDI-MS, NMR, and titration. The use of these endgroup-functionalized dendrimers as catalysts for the hydrolysis of 2,4-dinitrophenyl acetate is described. Molecular simulations provide a basis for interpreting the catalytic data.

Keywords : Dendrimer, Catalysis, Cooperativity, Hydrolysis.

Introduction

In this paper we describe the preparation, characterization, and catalytic activity of imidazole-modified dendrimers. The history of the use of imidazole-modified polymers for the catalytic hydrolysis of activated esters is quite rich. Particularly relevant to this work are the previous results of Klotz[1,2] and Overberger[3-5] who independently demonstrated that imidazole-modified polymers are capable of exhibiting cooperative catalysis in which two neighboring imidazole units served as general-acid/general-base catalysts. Overberger used primarily poly(vinyl imidazoles) while Klotz used primarily poly(ethylene imine) modified with imidazoles. In the case of poly(vinyl imidazole), the imidazole moieties are close enough together to function cooperatively with no further modifications. In the case of poly(ethylene imine), hydrophobic groups or strongly interacting substrates (such as sulfonates or carboxylic acids) are necessary to observe cooperativity. Imidazole-modified cyclodextrins[6,7] and protein loops[8] have also been used to rigidly hold imidazole units in close proximity for cooperative catalysis of activated esters and phosphodiesters.

In multi-imidazole general acid/general base catalytic systems, cooperativity is established if the rate of hydrolysis achieves a maximum when the solution pH equals the pK_a of the imidazole moieties. This occurs because the maximum concentrations of acid and base are simultaneously present under these conditions.

Dendrimers are a useful scaffold for designing catalytic systems. As the generation of a dendrimer increases, so does the endgroup density; therefore, moieties held at the dendrimer exterior may have a better chance to interact, enhancing the statistical probability of achieving cooperative effects. Several studies have investigated cooperative catalysis with dendrimers. Detty and coworkers observed order-of-magnitude increases in catalytic rate with increasing dendrimer generation for the oxidation of bromide by phenylseleno-modified poly(benzyl ether) dendrimers.[9,10] In these studies, the authors attribute the increased reaction rate to an increase in the density of selenium groups and a possible increase in selenium-selenium interactions, which would enhance catalysis.

*Author to whom correspondence should be addressed. e-mail: crooks@tamu.edu; fax: +1-979-845-1399; voice: +1-979-845-5629
[1]Present address: Naval Research Laboratory, Code 6177, Washington, DC 20375-5342, U.S.A

Though this hypothesis was not proven conclusively, the data suggested that this was the first example of positive-cooperative (an increase in rate due to cooperating subunits) interactions in modified dendrimers.

In another study, van Koten and coworkers noticed a decrease in catalytic rate due to neighboring catalytic Ni(II) groups of peripherally modified carbosilane dendrimers.[11] As the generation of dendrimer increased, the interaction of Ni groups resulted in the formation of Ni(III) groups and subsequent deactivation of the catalyst.

Finally, Jacobsen and coworkers have modified poly(amido amine) dendrimer endgroups with [Co(salen)] catalysts.[12] In these studies, modified dendrimers were better catalysts than monomeric or dimeric [Co(salen)] compounds, but interestingly, the low generation dendrimers were better catalysts than high-generation dendrimers for asymmetric ring-opening reactions of epoxides. Steric constraints of increasingly crowded high-generation dendrimers were thought to prohibit the interaction of some catalyst sites in the high-generation dendrimers.

Here, we hypothesized that imidazole-terminated dendrimers would promote catalytic hydrolysis of activated esters by a general acid/general base mechanism. Specifically, we thought that increasing the relative number density of imidazole groups on a dendrimer surface by increasing the dendrimer generation, and thereby decreasing the average distance between imidazole groups, it would be possible to observe cooperative catalytic effects. Accordingly, we prepared imidazole-terminated third- and fifth-generation poly(propylene imine) dendrimers (PPI-Im_{16} and PPI-Im_{64}, respectively). Surprisingly, no cooperative catalytic effects for the hydrolysis of 2,4-dinitrophenyl acetate were observed. A possible explanation for this result, based on molecular modeling, is proposed.

Experimental Section

Chemicals. Third- and fifth-generation amine-terminated poly(propylene imine) dendrimers (DSM Fine Chemicals, The Netherlands, PPI-$(NH_2)_x$, x = 16 and 64 for generations 3 and 5, respectively) were dried on a Schlenk line for 4 h prior to use. 4-Imidazole carboxylic acid (Aldrich, 98%), triphenylmethyl chloride (Aldrich, 98%), dicyclohexylcarbodiimide (DCC, Advanced Chemtech), hydroxybenzotriazole hydrate (HOBt, Advanced Chemtech), anhydrous dichloromethane (Aldrich, 99.8%), and trifluoroacetic acid (TFA, Acros, 99%) were also used as received. Benzoylated dialysis tubing (MWCO ~2000) (Sigma) and 2,4-Dinitrophenyl acetate (DNPA, Acros, 95%) were used as received.

Procedures. Triphenymethyl-protected 4-imidazole carboxylic acid (trityl-ImCOOH) was prepared using a literature procedure.[13] Briefly, 3.178 g of 4-imidazole carboxylic acid (0.0283 M) and 10 mL of anhydrous triethylamine were dissolved in 30 mL of anhydrous dimethyl formamide. The solution was stirred and 8.247 g (0.0295 M) of triphenylmethyl chloride was added. The solution was stirred overnight. The trityl-ImCOOH was extracted from chloroform/

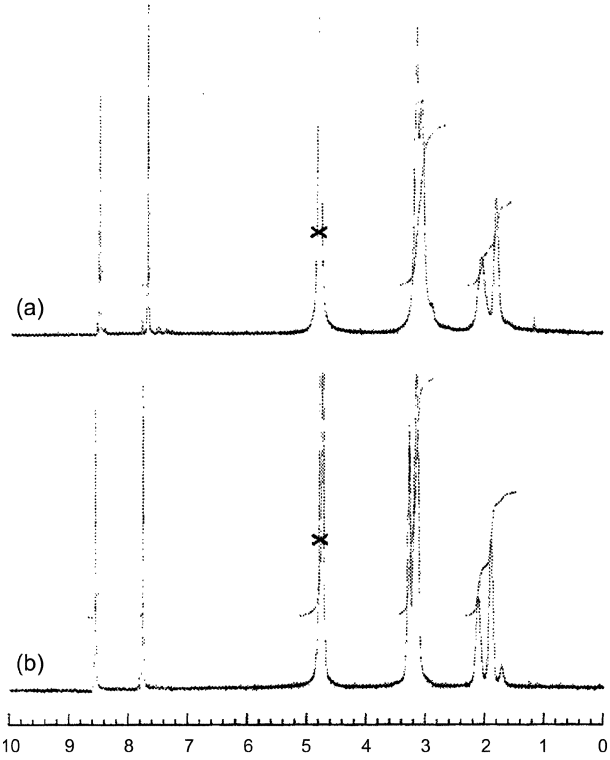

Figure 1. ^{1}H NMR (300 MHz) of (a) PPI-Im_{64} and (b) PPI-Im_{16}. (D_2O/10% DCl)

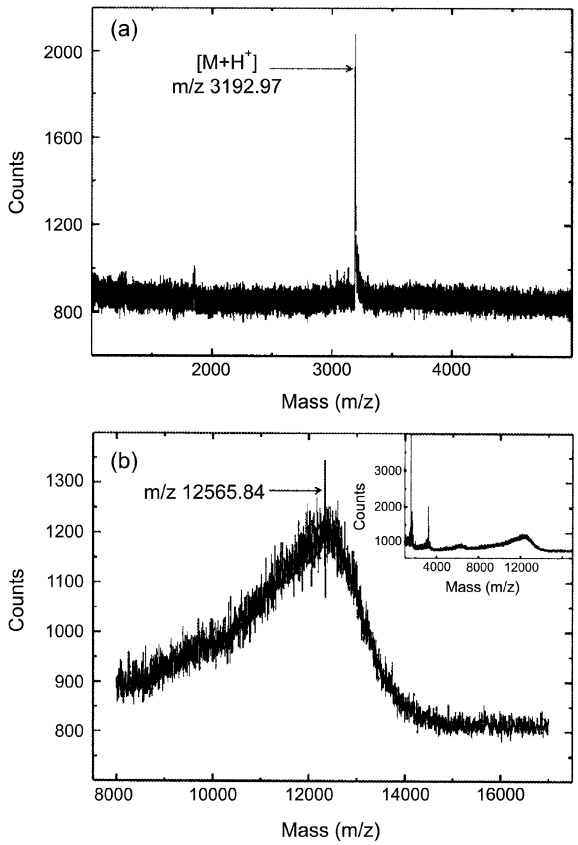

Figure 2. (a) MALDI-MS of PPI-Im_{16}; (b) MALDI-MS of PPI-Im_{64}, the inset shows the full MS spectrum and fragmentation observed.

water and washed extensively with hexanes, 10% citric acid, and brine. The chloroform was then evaporated, leaving 7.076 g (70% yield) of protected imidazole. ^{1}H NMR in $CDCl_3$ of the product displayed only a number of broad overlapping peaks arising from the aromatic protons in the region of 7-8 ppm. Chloroform was the only suitable deuterated solvent found, and because the solvent peak resides in this region (7.24 ppm) and due to the complex splittings observed, integration could not be performed. Accordingly, the product was used as recovered.

Dendrimers were functionalized by dissolving (separately) PPI-$(NH_2)_{16}$ (92.9 mg = 0.0551 mmol) or PPI-$(NH_2)_{64}$ (99.4 mg = 0.0139 mmol) in 10 mL of dry dichloromethane. Two solutions of 354 mg (1 mmol) of trit-ImCOOH, 230 mg (1.1 mmol) DCC, and 170 mg (1.1 mmol) HOBt were mixed briefly in anhydrous dichloromethane and then added to each solution of dendrimer. After stirring for 48 h, the solutions were concentrated, redissolved in chloroform, and subsequently washed with brine, and saturated aqueous Na_2CO_3. The chloroform layer was dried with anhydrous Na_2SO_4 and evaporated to yield trityl-imidazole modified PPI dendrimers.

The dendrimers were then dissolved in 1 : 1 CH_2Cl_2 : TFA, resulting in the formation of a viscous, insoluble polymer precipitate. This solution was extracted with water and the aqueous layer dialyzed (MWCO ~2000 dialysis tubing) against water for 2 days. The contents of the dialysis bag were then concentrated and dried on a Schlenk line overnight, yielding imidazole-modified PPI-Im_{16} and PPI-IM_{64}. MALDI-MS were recorded on a Voyager Elite XL MALDI time-of-flight mass spectrometer with a 337 nm pulsed nitrogen laser. 2',4',6'-Trihydroxyacetophenone (PPI-Im_{16}) and *trans*-3-indoleacrylic acid (PPI-Im_{64}) were used for MALDI matrices. ^{1}H NMR (Figure 1) (protons found/protons calculated based on a perfect, fully functionalized dendrimer), ^{13}C NMR and MALDI-TOF data (Figure 2) for PPI-Im_{16} and PPI-Im_{64} are provided below.

PPI-Im_{16}: (55.7 mg, 0.0174 mmol, 31% yield). ^{1}H NMR (300 MHz, D_2O/10% DCl): δ 2.00 (60/60H br, NCH_2CH_2-CH_2N, $NCH_2CH_2CH_2NH$, $NCH_2CH_2CH_2CH_2N$), 3.20 (115/116H br, $N(CH_2)_3$, CH_2NH), 7.81 (13/16H, s, Im), 8.62 (12/16H, s, Im); ^{13}C NMR (300 MHz, $CDCl_3$): δ ^{13}C NMR (75 MHz, D_2O/10% DCl): δ 18.3 ($NCH_2CH_2CH_2CH_2N$, $NCH_2CH_2CH_2N$), 22.6 ($NCH_2CH_2CH_2NHCO$), 36.2 (CH_2-CH_2NHCO), 48-51 ($N(CH_2)_3$), 120.1, 126.6, 135.0 (Im), 158.1 (*C*O); IR (KBr pellets): amide I 1660 cm^{-1}, amide II 1553 cm^{-1}; MS (MALDI-TOF) calculated for $C_{152}H_{240}N_{62}O_{16}$: 3192, found 3192.97 $[M + H]^+$.

PPI-Im_{64}: (151.1 mg, 0.0114 mmol, 83% yield). ^{1}H NMR (300 MHz, D_2O/10% DCl): δ 2.00 (252/252H br, NCH_2-CH_2CH_2N, $NCH_2CH_2CH_2NH$, $NCH_2CH_2CH_2CH_2N$), 3.20 (486/500H br, $N(CH_2)_3$, CH_2NH), 7.65 (49/64H, s, Im), 8.59 (54/64H, s, Im); ^{13}C NMR (75 MHz, D_2O/10% DCl): δ 18.2 ($NCH_2CH_2CH_2CH_2N$, $NCH_2CH_2CH_2N$), 22.5 (NCH_2CH_2-CH_2NHCO), 36.1 (CH_2CH_2NHCO), 48-51 ($N(CH_2)_3$), 119.9, 126.7, 135.0 (Im), 157.8 (*C*O); IR (KBr pellet): amide I 1664 cm^{-1}, amide II 1554 cm^{-1}; MS (MALDI-TOF) calculated for $C_{632}H_{1008}N_{254}O_{64}$: 13188, found 12565.8 (see text).

Molecular Modeling. Modeling was performed in a manner analogous to previous reports in the literature.[14-17] Molecular models were created using the Cerius^2 (version 4.0) software package (Molecular Simulations, Inc.; San Diego, CA). The DREIDING[18] force field version 2.21 was used for optimization and molecular dynamics simulations. Specifically, third- and fifth-generation PPI dendrimers were constructed from a model of the previous generation by adding the appropriate number of propyl amine branches. The SMART algorithm and standard convergence settings were used to energy minimize each generation. Molecular dynamics (MD) simulations were then performed by the NVT method (constant volume and temperature) using the Nosé temperature thermostat (0.01 ps relaxation) for 10 ps at 1000 K, followed by 250 ps at 300 K with a step size of 1 fs. The structures were again energy minimized. After obtaining models of each generation, all primary amines were functionalized with imidazole carboxylic acid groups, thereby creating models of the dendrimers of interest. Minimization and dynamics were performed again, exactly as described for the unmodified dendrimers. Static properties reported are calculated based on the final minimized structure. Radii of gyration, radial endgroup distributions, and carbonyl-carbonyl distances are calculated on the basis of the last 50 ps of the dynamics simulation, at which time equilibrium had been attained.

UV-Vis Spectroscopy. UV-vis measurements were made with a HP8453 UV-vis absorption spectrophotometer. Time-dependent measurements were recorded using the HP Chemstation Kinetics Analysis package. Measurements were made in polystyrene cells using a stirred and water-jacketed sample stage maintained at 23 ± 1 °C. Imidazole-modified

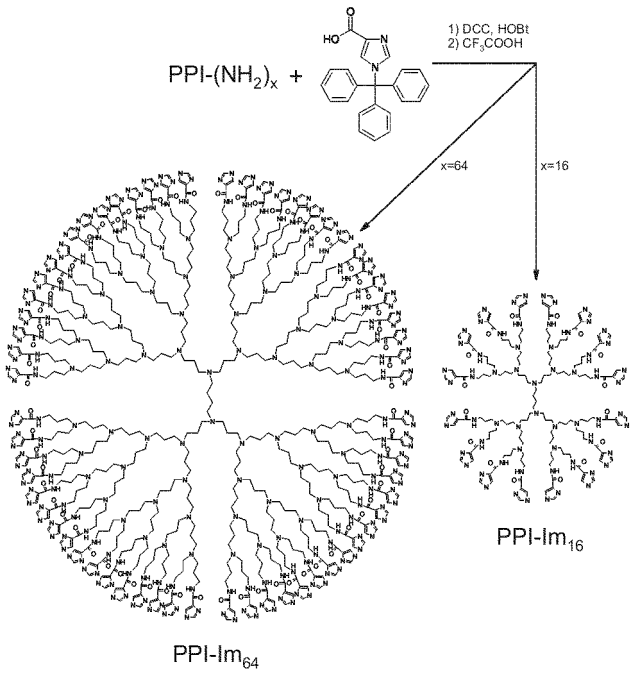

Figure 3. Synthesis of imidazole-terminated PPI dendrimers.

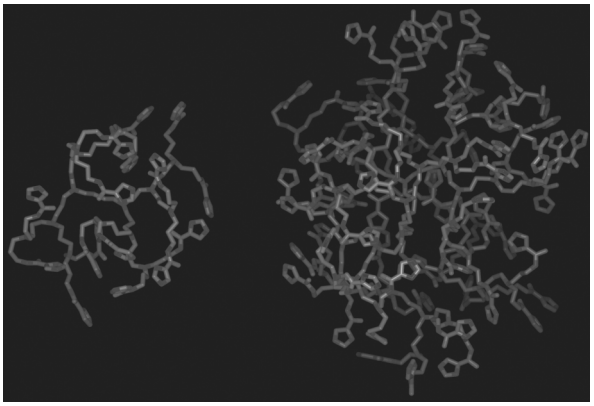

Figure 4. Final minimized structures of PPI-Im_{16} and PPI-Im_{64}. Structures were calculated using DREIDING forcefield.

dendrimer and imidazole solutions were prepared in H_2O (3.0 mL total volume) with an appropriate buffer (30 mM acetate buffers for pH < 6, 30 mM phosphate buffers for pH > 6). The ionic strength due to the buffer was 0.1 M. Background spectra were recorded, and then 30 μL of 2,4-dinitrophenyl acetate (DNPA) dissolved in acetonitrile was pipetted into the stirring solution. The initial concentration of DNPA was nominally 2.5×10^{-5} M, and the initial concentration of catalyst (imidazole endgroup) was nominally 3.5×10^{-4} M. Spectra were recorded every minute for 30 min following addition of DNPA. At the conclusion of the kinetic measurements 10 μL of concentrated NaOH were added to the solution and 30 min later the absorbance was recorded to obtain a value for A_∞ (absorbance at infinity).

Data were plotted as $-\ln(A_\infty - A_t)$ *vs*. time (where A_∞ is the measured absorbance at infinity and A_t is the absorbance at time t). This resulted in a straight line, the slope of which is the pseudo-first order rate constant, k_{meas}, of hydrolysis. The measured rate, k_{meas}, was corrected for water hydrolysis by subtracting the rate obtained in buffer solution with no catalyst present. Second-order rate constants, k_{cat}, were calculated by dividing the measured rate, k_{meas}, by the molar concentration of imidazole present in solution.

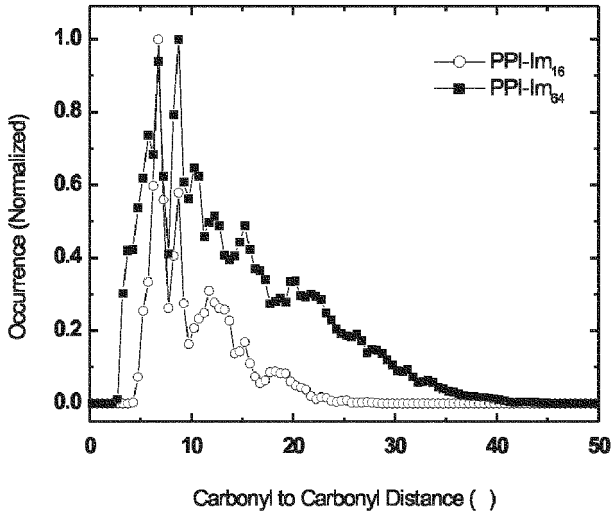

Figure 5. Measurement of carbonyl to carbonyl distance for PPI-Im_{16} and PPI-Im_{64}. Data are normalized to one at maximum.

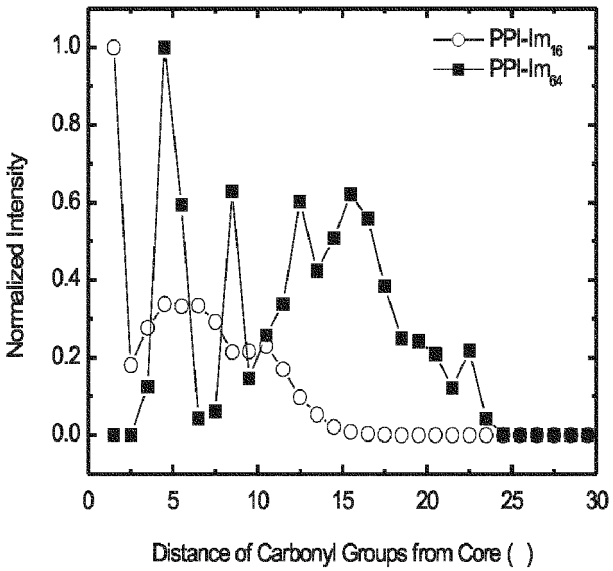

Figure 6. Measured distance of carbonyl groups from the core of the dendrimer.

pH Titrations. Titrations of PPI-$(NH_2)_x$, PPI-$(Im)_x$ (x = 16 or 64), and imidazole were carried out using a custom-built autotitrator. An appropriate amount of amine (~2.2 μM) was dissolved in 3.0 mL of water and the pH adjusted to below 3 with 238 mM HCl. A syringe pump (running at 0.2033 μL/s) titrated the solution with 0.1 M NaOH over a period of approximately 1 h. The pH was recorded with a Hanna pH 213 pH meter interfaced to a computer that recorded the pH at 1 point/s.

Results and Discussion

Standard peptide coupling protocols were used to synthesize imidazole-terminated third- and fifth-generation poly(propylene imine) dendrimers (PPI-Im_{16} and PPI-Im_{64}, respectively, Figure 3). A trityl-protected version of 4-imidazole carboxylic acid was chosen for coupling to the dendrimer to suppress possible inter-imidazole side reactions, or side reactions with unconsumed DCC that could arise from reactions with the secondary amine of the imidazole, leading to an ambiguous product. Additionally, this synthetic strategy will make it possible in the future to further modify the secondary amine in a manner that encourages substrate binding. Purification by dialysis resulted in loss of significant material in the case of PPI-Im_{16} but provided sufficiently pure materials without the need for chromatography.

Molecular models of the prepared materials were constructed and a dynamics simulation at 300 K was performed. The final minimized structures of PPI-Im_{16} and PPI-Im_{64} are shown in Figure 4. The calculated radii of gyration are 9.7 and 15.5 Å for the two models. The distances between

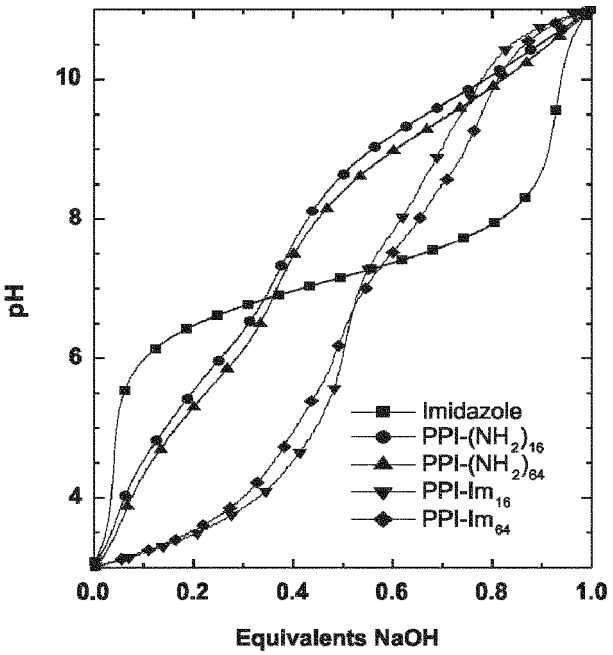

Figure 7. Titration (pH) of protonatable groups over the pH range 3-11.

neighboring carbonyl groups of imidazole modifiers was measured for the last 50 ps of the dynamics simulation in an effort to determine the effect of dendrimer generation on the endgroup-endgroup interactions (it should be noted, however, that no compensation for the effects of pH or solvent were included.) The results indicate that for PPI-Im_{64} approximately 10% of the measured distances are less than or equal to 5 Å, compared to about 4% for PPI-Im_{16} (Figure 5). This supports the idea that endgroup interactions increase as dendrimer generation increases. Additional measurements of the radial distribution of carbonyl groups from the central core of the dendrimer (Figure 6) show a distribution of endgroups throughout the volume of the dendrimer for both generations.

Experimental characterization of the two functionalized dendrimers was achieved with NMR, MALDI-MS, and FTIR. The extent of functionalization of dendrimers with imidazole can be estimated using ^{1}H NMR. By calculating and comparing the areas of integration of the peaks of the aromatic protons present on the imidazole ring (7.81 and 8.62 ppm for PPI-Im_{16}, 7.65 and 8.59 ppm for PPI-Im_{64}) versus the areas of integration from the dendrimer backbone peaks (2.0 ppm) (Figure 1) a high degree of functionalization for both dendrimer generations is obtained (81% for PPI-Im_{16} and 84% for PPI-Im_{64}). Additionally, ^{13}C NMR showed no evidence of free primary amines.

MALDI-MS of PPI-Im_{16} (Figure 2a) shows the presence of the $[M+H]^+$ ion at 3193 m/z and no other significant peaks. This mass corresponds to a 100% functionalized PPI-Im_{16} dendrimer, in contrast to the NMR finding of 81% functionalization. This disparity is likely due to either the inherent inaccuracy present in NMR measurements, or the presence of partially functionalized dendrimers that are not observed in the MALDI-MS. The MALDI-MS of PPI-Im_{64} (Figure 2b) is a broad ill-defined peak typical of high-generation dendrimers.[19,20] The inset shows the complete spectrum, which displays peaks at lower m/z, which are likely due to fragmentation of the dendrimer. The center of mass of the peak at 12,565 m/z is very close to the molecular mass (12,584) of a fully functionalized dendrimer in which the original dendritic starting material was missing 4 branches. This is significant because MALDI-MS of the starting PPI-$(NH_2)_{64}$ material is also a broad ill-defined peak whose center corresponds to starting material missing 3-4 branches.

FTIR of both materials confirmed formation of amide bonds as evidenced by the amide I and II stretches at ~1660 and ~1550 cm^{-1}.

Results of titrations of PPI-$(NH_2)_{16}$, PPI-$(NH_2)_{64}$, PPI-Im_{16}, PPI-Im_{64}, and imidazole are shown in Figure 7. Amine- and imidazole-terminated dendrimers are polyelectrolytes, and therefore the slopes of the titration curves do not break abruptly, making it difficult to determine the pK_a. However, this finding confirms that the amine groups on the surface of these dendrimers are in communication with one another. In contrast, the monomeric imidazole reveals a well-defined pK_a at approximately pH = 7.1, which is in good agreement with literature values.[21] Likewise, the shapes of the titration curves for the amine-terminated dendrimers are very similar to those previously reported,[22] with a half-neutralization point (the pH value necessary to deprotonate half of the amine residues (e.g. equiv. NaOH = 0.5)) at pH ~8.5. The half-neutralization point for the imidazole dendrimers is approximately 6.2, and the shape of the curve has the same features previously reported for histidine-modified polylysine: shallow slope in the pH range 3.0-4.5, then steeply increasing.[23]

The total number of amines in PPI-Im_{16} is 46 : 14 tertiary amines from the dendrimer interior, 16 secondary amines from imidazoles, and 16 tertiary amines from imidazoles. In imidazole monomers, the pK_a of the tertiary amine is ~14, so for the purposes of the data shown in Figure 7, which span a range of 3-11 pH units, protonation of the tertiary imidazoles can probably be neglected. Previous theoretical studies suggest that for primary amine-terminated PPI dendrimers, the intrinsic pK_a of the primary and tertiary amines do not differ from each other significantly. Instead, it is the electrostatic interactions between the shells (layers of concentric branches of the dendrimer) that give rise the apparent difference in pK_a values as determined from a pH titration curve.[22,24] Determination of the intrinsic pK_a, which is necessary for optimizing general acid/general base catalysis, is complicated because theoretical models for analyzing titration data are still controversial.[25] In this study, catalytic measurements were obtained over a broad pH range (pH = 5-9) in an effort to be certain that a catalytically efficient pK_a was encompassed. In previous studies of cooperative imidazole catalysis[6,7] it was found that a plot of the catalytic rate *vs.* pH results in a bell-shaped profile. The highest rate of catalysis occurs at the pK_a of the catalyst.

Catalytic measurements were obtained for the hydrolysis of 2,4-dinitrophenyl acetate (DNPA) in the presence and absence of imidazole-modified dendrimer. The rate of hydrolysis of DNPA in the dendrimer-free buffer was subtracted from that obtained in the dendrimer-containing solution to yield the rate resulting exclusively from the presence of the catalyst. This is important because even in the absence of catalysts, the rate of DNPA hydrolysis increases with pH. Rate measurements were obtained by dissolving the imidazole-modified dendrimer and substrate in water with an effective imidazole-to-substrate ratio of 10 : 1 and then monitoring the appearance of the hydrolysis product, dinitrophenolate, spectrophotometrically (Equation 1). The starting material, 2,4-dinitrophenyl acetate, absorbs at 243 nm, but after hydrolysis the product, 2,4-dinitrophenolate, absorbs at 360 nm.

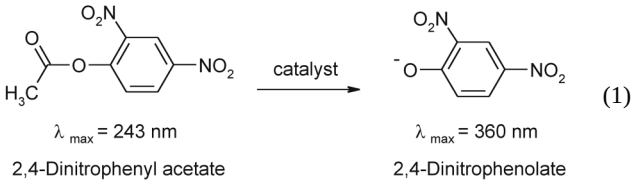

(1)

By recording the increase in absorbance at 360 nm or the decrease in absorbance at 243 nm as a function of time, kinetic data relating to the rate of reaction may be obtained. Nitrophenyl acetate is often chosen as the substrate for studies such as these, but we used DNPA primarily because the pK_a of the hydrolyzed dinitrophenolate is ~4.1, as compared to nitrophenolate which is ~7. Because the hydrolyzed anion is the species monitored spectrophotometrically, the lower pK_a of dinitrophenolate allows a broader pH range to be investigated.

Figure 8 shows the results of hydrolysis (uncorrected for background catalysis in the absence of the catalyst) of

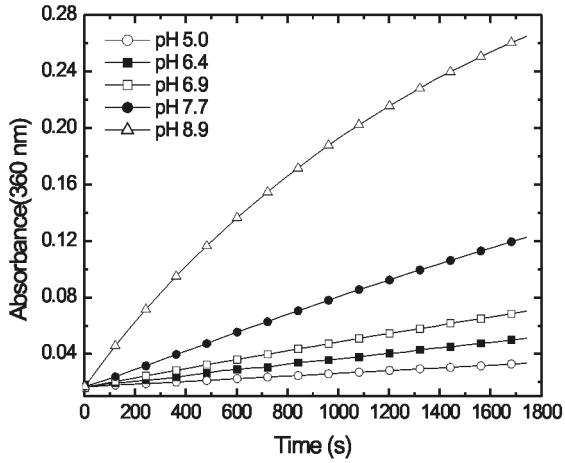

Figure 8. Measurement of hydrolysis of 2,4-dinitrophenyl acetate by PPI-Im_{16} as a function of time and pH (uncorrected for background hydrolysis by buffer). [DNPA] = 2.5×10^{-5} M, [PPI-Im_{16}] = 1.9×10^{-5} M ([I] = 3.0×10^{-4} M).

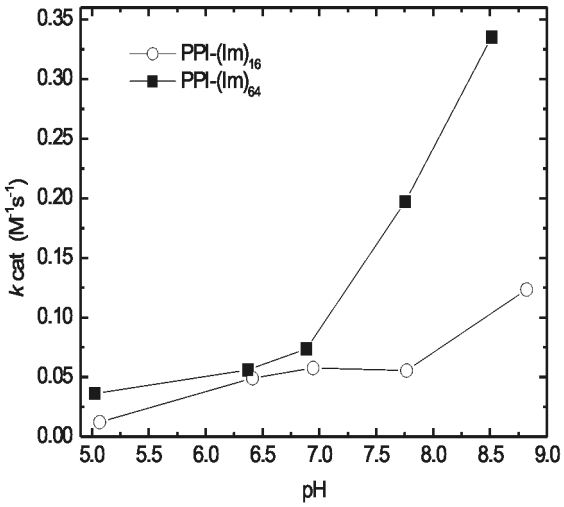

Figure 9. Catalysis (k_{cat}) of hydrolysis of 2,4-dinitrophenyl acetate as a function of pH for PPI-Im_{16} and PPI-Im_{64}.

DNPA in the presence of PPI-Im_{16} as a function of pH and time. Rates were determined by calculating the slope of $-\ln(A_\infty - A_t)$ (where A_∞ is the measured absorbance at infinity and A_t is the absorbance at time t) *vs.* time, after correcting for background hydrolysis from water and dividing by the molar concentration of imidazole present. The rates of hydrolysis of DNPA catalyzed by PPI-Im_{16} and PPI-Im_{64} are plotted in Figure 9.

The data indicate that the catalytic rates for hydrolysis of DNPA by imidazole-modified dendrimers are from 10-20 times lower compared to monomeric imidazole. For example, at pH 8.5 the following catalytic rates were observed: PPI-Im_{64}, 0.33 $M^{-1}s^{-1}$; PPI-Im_{16}, 0.10 $M^{-1}s^{-1}$, Imidazole, 4.3 $M^{-1}s^{-1}$. We believe this decrease is a consequence of the smaller number of basic sites on the imidazole dendrimers (compared to imidazole) at a particular pH. This in turn is a consequence of the polyprotic nature of the imidazole dendrimer and the corresponding differences in the titration curves. It should be noted, however, that the pK_a and reactivity of imidazole relative to a substituted imidazole (such as the amide substituted imidazoles appended to the dendrimer) is expected to be somewhat different due to electronic effects of the substituents. Therefore, the unsubstituted imidazole serves as a frame of reference for the imidazole-modified dendrimers, rather than as an exact model compound.

If cooperative catalysis were encouraged by the dendrimer scaffold, then the plot of k_{cat} *vs.* pH would be bell-shaped and have a maximum near the pK_a of the pendant imidazole groups. This is not the case for the data shown in Figure 9, however. Instead, the catalytic rate increases monotonically at higher pH, presumably due to simple base-catalyzed hydrolysis arising from either individual pendant imidazole groups or possibly unreacted primary amines present on the dendrimer. The same feature (rising rate with increasing pH) was observed when the hydrolysis was carried out with monomeric imidazole only.

Summary and Conclusions

Imidazole-modified dendrimers were synthesized, characterized, and used to establish whether or not positive cooperative effects between peripheral units on the dendrimer would enhance the catalytic rate for hydrolysis of DNPA. On the basis of pH-dependent measurements of the hyrolysis rate of DNPA in the presence of imidazole-modified dendrimers, however, there are no measureable positive cooperative effects attributable to the dendrimeric endgroups.

There are several possible explanations for the observed results. First, the dendrimers could aggregate, decreasing substrate access to imidazoles buried within the aggregates. Aggregation could occur in our experiments because the dendrimer concentrations were kept high to offset the significant background hydrolysis resulting from the basic buffer. However, we view this possibility as unlikely because all experiments were carried out in solutions containing 0.1 M salt, which is a condition known to reduce the likelihood of dendrimer aggregation.[19] An alternative explanation for the low observed catalytic activity, is that the pK_a of the imidazole units attached to dendrimers is outside the range of pH 5-9. However, it seems unlikely that the dendrimer attachment chemistry would result in a shift of more than one pH unit away from the pK_a of monomeric imidazole (~7).

There are two factors that most likely account for the absence of cooperative catalysis. The first involves the geometric and steric properties of the dendrimer framework. It is likely that imidazoles are not distributed exclusively on the periphery of the dendrimer, but rather distributed throughout the volume of the dendrimer (this is supported by the molecular models, Figure 6). We hypothesize that in the absence of a strong driving force for association of endgroups, such as in the case of the π-stacking of pyrene molecules observed in our previous study of dendrimer-based cooperativity,[26] the pendant imidazole groups are not sufficiently close together to achieve cooperativity. This problem is exacerbated if imidazole functional groups appended to the periphery of the dendrimer fold back into the dendrimer interior. This level of structural flexibility has been observed by others.[27]

The second factor concerns the driving force for substrate-catalyst association. In previous cooperative catalytic systems using multiple imidazole species, the presence of a hydrophobic pocket has been shown to increase the rate of hydrolysis by increasing substrate-catalyst association. For example, imidazole-modified cyclodextrins have been shown to be able to make use of both the hydrophobic cavity present in cyclodextrins and the close proximity of imidazoles attached to the cyclodextrin ring.[6,7] Imidazole-modified polymers containing co-polymerized alkyl substituents[4] have also been shown to increase substrate-catalysts association (with hydrophobic substrates), presumably through hydrophobic interactions with the appended alkyl groups. A key aspect of this work is the development of a method for efficiently attaching protected imidazole groups to the dendrimer exterior. In the future this will allow us to incorporate substrate binding functionality into the dendrimers and thereby test this hypothesis.

Most likely it is a combination of these last two factors, namely geometric considerations of the dendrimer structure and weak substrate-catalyst association, that have resulted in the low catalytic rates and absence of cooperativity observed in the catalytic measurements of the imidazole-modified dendrimers described herein. Additional experiments are planned to better understand these factors.

Acknowledgment. The authors gratefully acknowledge the American Chemical Society Petroleum Research Fund (ACS-PRF#35756) for financial support. We also thank Dr. Lisa M. Thomson and the Texas A&M Laboratory for Molecular Simulation for assistance with calculations and the use of software and computing time.

References

1. Klotz, I. M. *Adv. Chem. Phys.* **1978**, *39*, 109-176.
2. Nango, M.; Klotz, I. M. *J. Polym. Sci., Polym. Chem. Ed.* **1978**, *16*, 1265-1273.
3. Overberger, C. G.; Salamone, J. C. *Acc. Chem. Res.* **1969**, *2*, 217-224.
4. Overberger, C. G.; Kawakami, Y. *J. Poly. Sci.: Poly. Chem. Ed.* **1978**, *16*, 1237-1248.
5. Tomko, R.; Overberger, C. G. *J. Poly. Sci.: Poly. Chem. Ed.* **1985**, *23*, 265-277.
6. Breslow, R.; Schmuck, C. *J. Am. Chem. Soc.* **1996**, *118*, 6601-6605.
7. Breslow, R.; Dong, S. D. *Chem. Rev.* **1998**, *98*, 1997-2011.
8. Nilsson, J.; Baltzer, L. *Chem. Eur. J.* **2000**, *6*, 2214-2220.
9. Francavilla, C.; Bright, F. V.; Detty, M. R. *Org. Lett.* **1999**, *1*, 1043-1046.
10. Francavilla, C.; Drake, M. D.; Bright, F. V.; Detty, M. R. *J. Am. Chem. Soc.* **2001**, *123*, 57-67.
11. Kleij, A. W.; Gossage, R. A.; Gebbink, R. J. M. K.; Brinkmann, N.; Reijerse, E. J.; Kragl, U.; Lutz, M.; Spek, A. L.; van Koten, G. *J. Am. Chem. Soc.* **2000**, *112*, 12112-12124.
12. Breinbauer, R.; Jacobsen, E. N. *Angew. Chem. Int. Ed.* **2000**, *39*, 3604-3607.
13. Ding, C. a.; Batorsky, R.; Bhide, R.; Chao, H. J.; Cho, Y.; Chong, S.; Gullo-Brown, J.; Guo, P.; Kim, S. H.; Lee, F.; Leftheris, K.; Miller, A.; Mitt, T.; Patel, M.; Penhallow, B. A.; Ricca, C.; Rose, W. C.; Schmidt, R.; Slucsarchyk, W. A.; Vite, G.; Yan, N.; Manne, V.; Hunt, J. T. *J. Med. Chem.* **1999**, *42*, 5241-5253.
14. Miklis, P.; Cagin, T.; Goddard, W. A. *J. Am. Chem. Soc.* **1997**, *119*, 7458-7462.
15. Cavallo, L.; Fraternali, F. *Chem. Eur. J.* **1998**, *4*, 927-934.
16. Cagin, T.; Wang, G.; Martin, R.; Breen, N.; Goddard, W. A. *Nanotechnology* **2000**, *11*, 77-84.
17. Cagin, T.; Wang, G.; Martin, R.; Zamanakos, G.; Vaidehi, N.; Mainz, D. T.; Goddard, W. A. *Comp.* **2001**, *11*, 329-343.
18. Mayo, S. L.; Olafson, B. D.; Goddard, W. A. *J. Phys. Chem.* **1990**, *94*, 8897-8909.
19. Baker, W. S.; Lemon, B. I.; Crooks, R. M. *J. Phys. Chem. B* **2001**, *105*, 8885-8894.
20. Woller, E. K.; Cloninger, M. J. *Biomacromolecules* **2001**, *2*, 1052-1054.
21. Sundberg, R. J.; Martin, B. R. *Chem. Rev.* **1974**, *74*, 471-517.
22. van Duijvenbode, R. C.; Borkovec, M.; Koper, G. J. M. *Polymer* **1998**, *39*, 2657-2664.
23. Benns, J. M.; Choi, J.; Mahato, R. I.; Park, J.; Kim, S. W. *Bioconj.*

Chem. **2000**, *11*, 637-645.
24. Koper, G. J. M.; van Genderen, M. H. P.; Elissen-Román, E.; Baars, M. W. P. L.; Meijer, E. W.; Borkovec, M. *J. Am. Chem. Soc.* **1997**, *119*, 6512-6521.
25. Sun, L.; Crooks, R. M. *J. Phys. Chem. B*, in press.
26. Baker, L. A.; Crooks, R. M. *Macromolecules* **2000**, *33*, 9034-9039.
27. Bosman, A. W.; Janessen, R. A. J.; Meijer, E. W. *Chem. Rev.* **1999**, *99*, 1665-1688.